Proceedings of 10th International Conference on Precision, Meso, Micro and Nano Engineering (COPEN 10)
December 07 – 09, 2017, Indian Institute of Technology Madras, Chennai – 600 036 INDIA

Evaluation of Wire Electro Discharge Machining Characteristics of $Ti_{50}Ni_{45}Co_5$ Shape Memory Alloy

Hargovind Soni*, Narendranath S and Ramesh M R

Department of Mechanical Engineering
National Institute of Technology Karnataka, Surathkal - 575025, INDIA

Abstract

The present study investigates the influence of wire electro discharge machining characteristics on $Ti_{50}Ni_{45}Co_5$ shape memory alloy. Machining of $Ti_{50}Ni_{45}Co_5$ alloy has been carried using Taguchi design of method creating L-9 orthogonal array and the process parameters are optimized through principal component analysis (PCA) based Grey relational analysis (GRA) technique. Moreover, characterization of the machined surface is performed with respect to microstructures and microhardness analysis. The machined surface is harder and microstructure exhibit microcracks, microglobules and melted drops.

Keywords: Shape memory alloy, wire electro discharge machining, microstructure, microhardness.

1. INTRODUCTION

Due to excellent biocompatibility, TiNi based shape memory alloys are used for biomedical applications such as bone staple, stone extraction baskets, cardio-vascular stents, catheter guide wires and other biomedical devices [1]. To further expand their use in several other applications, additional alloying elements are to be used. Adding the third element in TiNi alloys by decreasing Ti or Ni has an extensive effect on their phase transformation behavior and properties of the material [2, 3]. Addition of Co in TiNi which replaced Ni improved their physical (shape memory effect, pseudoelasticity, transformation temperature and biocompatibility) and mechanical (strength, fatigue and cyclic loading and damping capacity) properties which make it more suitable for biomedical applications like staples for clinical joining of mandible and face bone fractures [4, 5]. Machining of these materials is very difficult through conventional machining because conventional machining may affect their internal properties, therefore non-conventional machining processes are more suitable. Wire electro discharge machining (WEDM) is one of the non-conventional machining processes, which is used in manufacturing industries to machine conductive and semi conductive materials with complex shapes [6]. The important input process parameters of WEDM process are pulse on time, pulse off time and servo voltage. Several researchers have optimized the WEDM input process parameters using several combinations of optimization techniques. Elsen and Ramesh [7] optimized the WEDM process parameters using hybrid combination of RSM and GRA techniques for the responses of hardness and compressive strength of zirconia reinforced alumina. Dhuria et al. [8] have optimized input process parameters of ultrasonic machining of Ti-6Al-4V alloy using a combination of GRA and Entropy measurement. The aim of present study is that to find the best combination of process parameters for the machining of $Ti_{50}Ni_{45}Co_5$ alloy with higher material removal rate (MRR) with lower surface roughness (SR) using principal component analysis based Grey relational analysis technique. Machined surface characterization will be carried out with respect microstructures and microhardness at optimized process parameters.

2. MATERIALS AND METHODS

$Ti_{50}Ni_{45}Co_5$ SMAs has been developed through a vacuum arc melting. The material homogeneity is achieved by carrying out melting for six times successively, followed by casting into rectangular blocks of size 50mm x 12mm x 10mm. WEDM (Model Electronica ELPULS15 CNC) is used for profile cutting of bone staple at optimized process parameters. Table 1 represents the selected process parameters and their levels. The L-9 orthogonal array was generated by Taguchi design method for the machining on WEDM which is represented in Table 2. The Material removal rate is calculated by equation 1 [9] and surface roughness is measured by Telly surf (Mitutoyo) roughness tester. The roughness of each machined surface has been measured at three different locations under the tester parameters as cutoff length 0.8 mm and an evaluation length of 3 mm and the stylus speed of 0.25 mm/s and the average surface roughness (Ra) is reported in the present study.

MRR = cutting speed (mm/min) x width of cut (mm) x height of work piece (mm) ---------- (1)

Where, width of cut (mm) = 2 x spark gap + diameter of wire (mm)

The input process parameters were optimized for each alloy through a hybrid combination of grey relation analysis (GRA) and principle components analysis (PCA) optimization technique. GRA, which requires limited information to estimate the behavior of an uncertain system and discrete data problem. If the sequence range is large, the factors are effaceable therefore data pre-processing is an important steps to manage the factors of GRA. For the data pre-processing, there are two conditions of normalization in the present study namely higher the better which will be used in the normalization of MRR and another one lower the better for normalization of SR values of each specimen of both alloys. Table 2 indicates the two conditions of normalization with equations 2 and 3.The goals of PCA are to take out the most significant information from the data, compress the size of the data set by observance only this significant, simplify the justification of the data set, and study the structure of the explanation and the variables. A detail of these combinations of optimization techniques is available in the author's earlier research work [10]. The microstructure analysis of machined surface has been carried out by using 'JEOL JSM-638OLA' scanning electron microscopy (SEM). Microhardness measurement was made through 'MVH-S-

ISBN: 978-93-80689-28-9

AUTO' OMNITECH microhardness tester with 300g load and 15s dwell time.

Table 1: Input process parameters and their levels

Process parameters	Levels		
	1	2	3
Pulse on Time (T_{on})	115 (µs)	120 (µs)	125 (µs)
Pulse off time (T_{off})	30 (µs)	35 (µs)	40 (µs)
Servo voltage (SV)	40 V	45 V	50 V

Table 2 Conditions of normalization

Conditions	Equations
Lower is better	$X_i^*(k) = \frac{X_i(k) - \min X_i(k)}{\max X_i(k) - \min X_i(k)}$.(2)
Higher is better	$X_i^*(k) = \frac{\max X_i(k) - X_i(k)}{\max X_i(k) - \min X_i(k)}$.(3)

where i = 1, 2n, k = 1, 2, y, p; (k) is the normalized value of the k^{th} element in the i^{th} sequence, max X_i (k) is the largest value of X_i (k), and min X_i (k) is the smallest value of X_i(k), n is the number of experiments and p is the number quality characteristics.

3. RESULTS AND DISCUSSION

Measured values of MRR and SR are given in Table 3 while Table 4 exhibits all calculation of optimization techniques. Based on the maximum value of GRG, Run no. 8 found to be the best combination of process parameters (Table 3).

Table 3: L-9 orthogonal array and outputs

Run No.	Ton	Toff	SV	MRR (mm^3/min)	SR (Ra)
1	115	30	40	6.9784	2.343
2	115	35	45	4.23475	2.040
3	115	40	50	3.4268	2.056
4	120	30	45	7.7298	2.300
5	120	35	50	5.71285	2.260
6	120	40	40	5.4119	2.393
7	125	30	50	9.51665	2.423
8	125	35	40	10.0823	2.876
9	125	40	45	7.35267	2.536

3.1 Effects of input process parameters on output responses

Fig. 1a exhibits the effect of input process parameters on material removal rate where MRR is increasing with increase in pulse on time. This is because at high pulse on time, spark intensity is high there by more thermal energy is available to remove the material from the work surface which results in less time required for removal of material from the workpiece surface; hence it is leading to high MRR. MRR decreases with high pulse off time which is due to decrease in spark intensity hence less amount of material removes from the workpiece surface comparatively leading to low MRR as can be seen in Fig 1a. MRR decreases at high servo voltage because increase in servo voltage results in larger spark gap thereby reducing the spark intensity and eventually lesser amount of material is removed from the surface of the workpiece. Similar kind of result has been reported by Sivaprakasam et al. [11] during the wire electro discharge machining of A413-B4C. It has been observed from Fig. 1b that surface roughness increase with the increase in pulse on time because when it removes more amount of material, some of the molten material are flushed off by dielectric fluid as the rate of materials removal is high and remaining molten metal solidify on machined surface and it forms craters and micro globules leading to higher surface roughness which can be seen in Fig. 2. Surface roughness slightly increases up to 35 µs but it decreases with increase in pulse off time this may be because, at high pulse off time most of the molten metal is flushed away from the machined surface and reduce the formation of craters and micro globules hence leading to low surface roughness. Lower surface roughness has been recorded at high servo voltage. This is because less amount of material is melted on the machined surface; this can be easily flushed away from the machined surface through dielectric fluid leading to low surface roughness. Soni et al. [12] observed similar results during the wire electro discharge machining of TiNiCo alloys.

3.2 Microstructure analysis of machined surface

Microstructure analysis has been carried out on machined surface at optimized process parameters. Micro globules, cracks, recast deposition; melted drops, blow holes and craters were noticed on the machined surface. Crater, more melted drops and micro globules were observed on the machined surface which is seen in Fig. 2. This may be due to the lower servo voltage resulting in higher surface roughness due to more intense spark discharge on the machining surface that leads to the formation of larger and abrupt crater along with faster resolidification of molten material by dielectric quenching. However this is not sufficient enough to produce the required localized pressure which can splash all the molten material from the machining zone which is to be washed away due to flushing pressure. But some of the molten materials remain attached to the machined surface which tends to entrap some air bubbles and thus produces microvoids and micro globules on the machined surface. Recast deposition is observed on the machined surface due to higher pulse on time because at high pulse on time, more amount of thermal energy is transferred to the material which results in the melting of more amount of material from the workpiece. This, in turn, contributes to the increase in size of the craters and melting drops formed on the machined surface and consequently produces a rough surface on the machined components. Similar work has been reported by Sharma et al. [13] during wire electro discharge machining of Inconel 706.

3.3 Microhardness analysis

Microhardness analysis has been carried out across the cross section up to 100µm from the machined surface. During the machining process three kinds of layers are generated on the machined surface such as recast layer, heat affected zone and converted layer [14]. Recast layer near the cutting edge was considered as a starting point (0µm) and microhardness is measured towards the base material as shown Fig. 3.

Microhardness is found to be more in recast layer zone due to formation of surface oxides. Below the recast layer microhardness reduces in the heat affected zone. Beneath the heat affected zone converted layer is having comparatively less microhardness because converted layer is not much affected during WEDM process hence hardness of this zone is almost equal to hardness of base material. Similar kind of work is presented by Soni et al. [12] during wire electro discharge machining of TiNiCo shape memory alloy.

Table 4: optimization procedure for optimal process parameters

Run No.	Nor. MRR	Nor. SR	Dev. MRR	Dev. SR	GRC MRR	GRC SR	GRG	Rank
1	0.533633837	0.301219512	0.46636616	0.69878	0.517402222	0.41709054	0.467059	5
2	0.121395838	0.346341463	0.87860416	0.653659	0.362685689	0.43340381	0.397886	8
3	0	0	1	1	0.333333333	0.33333333	0.3332	9
4	0.646532943	0.297560976	0.35346706	0.702439	0.585845693	0.4158215	0.500633	4
5	0.343482834	0.248780488	0.65651717	0.75122	0.432332537	0.39961014	0.415805	7
6	0.298264593	0.41097561	0.70173541	0.589024	0.416064965	0.45912654	0.437421	6
7	0.915010142	0.447560976	0.08498986	0.552439	0.854715673	0.47508691	0.664635	2
8	1	1	0	0	1	1	0.9996	1
9	0.58986853	0.585365854	0.41013147	0.414634	0.54937118	0.54666667	0.5478	3

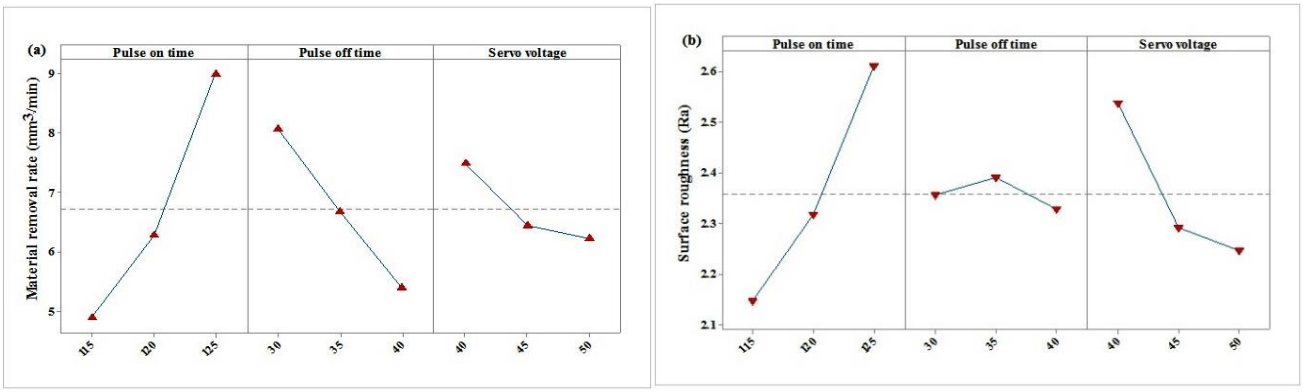

Figure 1 Effect of input process parameters Vs. (a) MRR and (b) SR

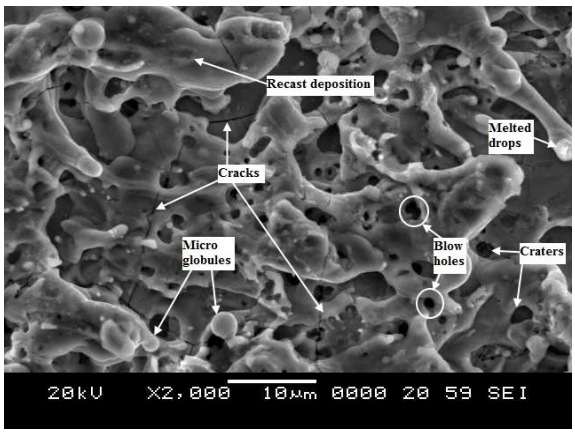

Figure 2 Microstructure analysis of machined surface at run no. 8

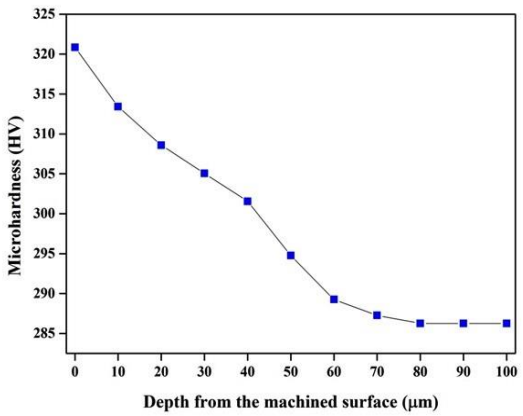

Figure 3 Microhardness analysis of near machined surface

4. CONCLUSIONS

By using vacuum arc meting furnace $Ti_{50}Ni_{45}Co_5$ shape memory alloy was fabricated and machined through wire electro discharge machining process. Following conclusions can be drawn:

- 125µs pulse on time, 35µs pulse off time and 40V servo voltage are found as the best combination of process parameters which are optimized through multi-objective optimization techniques.

- Material removal rate and surface roughness increase with increase in pulse on time and decrease with increase in pulse off time and servo voltage.

- Mirco globules, cracks, recast deposition, melted drops, blow holes and craters were noticed on machined surface. crater, more melting drops and micro globules are found the machined surface due to higher pulse on time and lower servo voltage.

- Harder surface has been noticed near the machined surface in recast layer zone due to the formation of oxides.

ACKNOWLEDGEMENT

The authors sincerely acknowledge the financial support from the Department of Science and Technology (DST), Government of India, bearing project reference no. SB/S3/MMER/0067/2013.

References

[1] Nolan, M. and Tofail S.A.M. Density functional theory simulation of titanium migration and reaction with oxygen in the early stages of oxidation of equiatomic NiTi alloy. *Biomaterials*, **31** (2010) 3439–48.

[2] Zheng Y.F., Zhang B.B., Wang B.L. Wang YB, Li L, Yang QB, et al. Introduction of antibacterial function into biomedical TiNi shape memory alloy by the addition of element Ag. *Acta Biomaterials*, **7** (2011) 2758–2767.

[3] Elahinia, M.H., Hashemi, M., Tabesh, M., Bhaduri S.B. Manufacturing and processing of NiTi implants: A review. *Progress in Material science*, **57** (2012) 911–946.

[4] Lekston, Z., Stroz, D., Drusik-Pawlowska, M.J. Preparation and characterization of nitinol bone staples for cranio-maxillofacial surgery. *Journal of material engineering performance*, **21** (2012) 2650–2656.

[5] Wever, D.J., Veldhuizen, A.G., Sanders, M.M., Schakenraad, J.M., Van Horn, J.R. Cytotoxic, allergic and genotoxic activity of a nickel-titanium alloy. *Biomaterials*, **18** (1997) 1115–1120.

[6] Kumar, A., Kumar, V., Kumar, J. Multi-response optimization of process parameters based on response surface methodology for pure titanium using WEDM process. *The International Journal of Advanced Manufacturing Technology*, **68** (2013) 2645–2668.

[7] S.R. Elsen, T. Ramesh, Optimization to develop multiple response hardness and compressive strength of zirconia reinforced alumina by using RSM and GRA. *Int. J. Refract. Met. Hard Mater*. **52** (2015) 159–164.

[8] G.K. Dhuria, R. Singh, A. Batish, Application of a hybrid Taguchi-entropy weight-based GRA method to optimize and neural network approach to predict the machining responses in ultrasonic machining of Ti–6Al–4V. *J. Brazilian Soc. Mech. Sci. Eng.* (2016).

[9] Manjaiah, M., Narendranath, S., Basavarajappa, S., Gaitonde, V.N. Effect of electrode material in wire electro discharge machining characteristics of $Ti_{50}Ni_{50-x}Cu_x$ shape memory alloy. *Precision Engineering*, **41** (2015) 68–77.

[10] Soni, H., Majhi, S.K. Multi-response optimization of EDM using Grey-PCA Approach. In Proceedings of *International Conference on Advanced Research in Mechanical Engineering*, **21stApril-2013**, Coimbatore, 1–5.

[11] Sivaprakasam, P., Hariharan, P., Gowri, S. Optimization of Micro-WEDM Process of Aluminum Matrix Composite (A413-B 4 C): A Response Surface Approach. *Materials and Manufacturing Process*, **28** (2013) 1340–1347.

[12] Soni, H., Sannayellappa, N., Motagondanahalli, Rangarasaiah, R. An experimental study of influence of wire electro discharge machining parameters on surface integrity of TiNiCo shape memory alloy. *Journal of material research*, **32** (2017) 1–9.

[13] Sharma, P., Chakradhar, D., Narendranath, S. Evaluation of WEDM performance characteristics of Inconel 706 for turbine disk application. *Materials and Design*, **88** (2015) 558–566.

[14] Choudhary, R., Kumar, H., Garg, R.K. Analysis and evaluation of heat affected zones in electric discharge machining of EN-31 die steel. *Indian Journal of Engineering and Material Science*, **17** (2010) 91–98.